

Improving Lane Detection Generalization: A Novel Framework using HD Maps for Boosting Diversity

Daeun Lee^{1,2}, Minhyeok Heo¹ and Jiwon Kim^{1*}

Abstract—Lane detection is a vital task for vehicles to navigate and localize their position on the road. To ensure reliable results, lane detection algorithms must have robust generalization performance in various road environments. However, despite the significant performance improvement of deep learning-based lane detection algorithms, their generalization performance in response to changes in road environments still falls short of expectations. In this paper, we present a novel framework for single-source domain generalization (SSDG) in lane detection. By decomposing data into lane structures and surroundings, we enhance diversity using High-Definition (HD) maps and generative models. Rather than expanding data volume, we strategically select a core subset of data, maximizing diversity and optimizing performance. Our extensive experiments demonstrate that our framework enhances the generalization performance of lane detection, comparable to the domain adaptation-based method.

I. INTRODUCTION

Lane detection is a fundamental task in autonomous driving. By detecting lane markings on the road, autonomous vehicles can localize their position and identify drivable spaces, which provide fundamental information for safe operation on the road. Recently, thanks to advancements in deep learning, most studies have shifted from using traditional hand-crafted features to employing a data-driven approach, such as deep neural networks.

Nevertheless, data-driven lane detection algorithms still suffer from a performance degradation when tested on unseen or out-of-distribution data. The fundamental assumption of the data-driven approach is that the target data follows similar statistics to the training data [1]. As demonstrated in Fig. 1 (a), however, lane detection datasets typically vary due to various factors, such as camera mounting positions, road widths, capture times, and even country-specific lane marking standards. Such discrepancies between the source and target datasets result in a severe performance decrease as shown in Fig. 1 (b). Notably, we observed that the performance decrease between datasets is more noticeable not only when lane structures change (e.g., no lanes or curves) but also during transitions like day-to-night shifts, which notably impact the background surroundings compared to typical scenes.

¹D. Lee, M. Heo and J. Kim are with NAVER LABS, Seongnam-si, Gyeonggi-do, S. Korea [daeun.lee, heo.minhyeok, gl.kim]@naverlabs.com

²D. Lee is with Department of Statistics, Korea University, Seoul, S. Korea goodgpt@korea.ac.kr

[†]D. Lee was with NAVER LABS as a research intern when conducting this work.

*Corresponding author.

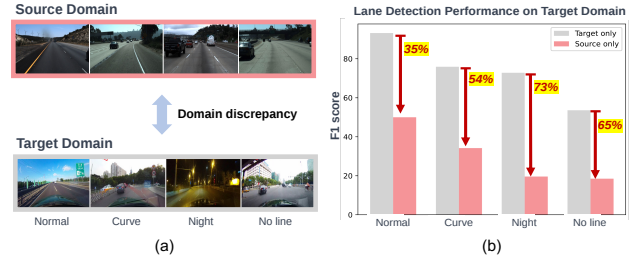


Fig. 1: Performance degradation by domain discrepancy. (a) Example images of source and target domains and (b) performance of the state-of-the-art lane detection model [2] on the target domain, still revealing significant challenges due to domain differences.

Recent studies [3, 4, 5, 6, 7] have attempted to address this performance degradation by incorporating additional data. These approaches include domain adaptation, which involves making use of a limited number of data samples from the target domain, and domain generalization, which leverages data from multiple source domains. However, in realistic autonomous driving scenarios, it is technically impossible to obtain even a small number of data samples from the target domain, as the target domain cannot be predetermined. Additionally, collecting data from numerous regions may have practical limitations. Therefore, for the lane detection task, it is essential to achieve generalization solely relying on a single-source domain without any prior information about the target domain.

In the context of single-source domain generalization (SSDG), it is imperative to obtain domain-invariant features, which necessitates a sufficiently diverse set of source domain data. Furthermore, controlling the augmentation of diversity within a constrained dataset helps the model concentrate on task-specific features. For instance, if there are data pairs with identical surrounding conditions (background, weather, obstacles, etc.) but varying lane structures, it is conceivable that the model will be trained to progressively disregard the influence of the surroundings. However, unfortunately it is practically impossible to acquire data with different lane structures while maintaining the same surrounding conditions.

In this paper, we propose a novel training framework for generalizing a lane detection model using only a single-source domain. Firstly, to do this, we decompose the lane detection data into two key elements: lane structures and surroundings. We achieve domain generalization performance

optimized by increasing diversity in each element. To enhance diversity in lane structures, we utilize High-Definition (HD) maps with various lane and road information. Additionally, we employ generative models to augment diversity in surroundings. In conclusion, rather than indiscriminately increasing the data, we present a data selection method by identifying a core set among the augmented data, where diversity is maximized.

The main contributions of the paper can be summarized as follows:

- We propose a novel training framework designed to generalize a lane detection model utilizing a single-source domain, addressing the domain generalization challenge in the context of realistic autonomous driving scenarios.
- We enhance domain generalization performance by systematically increasing diversity in two fundamental elements of lane detection data: lane structures and surroundings. We leveraged HD maps and generative models to enhance diversity in each element.
- Diverse experimental validations have demonstrated that the proposed training framework outperforms domain adaptation techniques without any prior target domain information.

II. RELATED WORK

A. Domain Adaptation for Lane Detection

Unsupervised Domain Adaptation(UDA) [8, 9, 10, 11] has been primarily adopted as a methodology for bridging domain discrepancy that occurs between different domains. In fact, it allows access to unlabeled target domains in the model learning process. Current research for domain adaptation in lane detection can be largely categorized into (i) Sim-to-Real and (ii) Cross-domain adaptation.

(i) **Sim-to-Real domain adaptation** is a field that adapts simulated data generated by gaming engines to the real world. Their main goal is to bridge the domain gap between photorealistic synthetic images and real-world data. ADA [12] utilizes adversarial discriminative and generative methods for adapting to the target domain, and UNIT [13] utilizes cycle-GAN-based methods.

(ii) **Cross-domain adaptation** is a method for narrowing the domain gap that occurs in two different driving environments. MLDA [14] is the first paper to point out the cross-domain discrepancy among CULane and TUSimple datasets. They solve this domain gap with a framework based on self-training. In particular, the setting of MLDA is also a form of cross-evaluation with only one source domain. However, the biggest difference from our framework is that they use RGB images of the target domain in their adaptation process.

Given that both of the above fields require target domain information, it is difficult to apply it in a realistic driving environment.

B. Single-Source Domain Generalization

Unlike Multi-Source Domain Generalization(MSDG), Single-Source Domain Generalization(SSDG) [15, 16, 17]

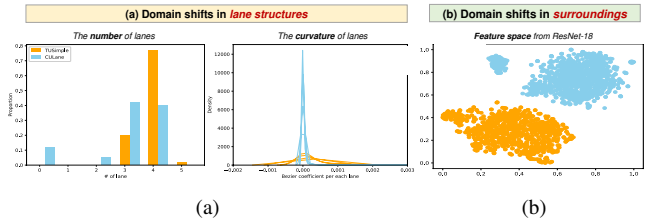


Fig. 2: **Domain discrepancy in lane detection.** We categorized the cause of domain discrepancy in lane detection. (a) The difference in the number of lanes and curvatures shows a clear discrepancy in lane structures. (b) Judging from the t-SNE [30] analysis, the contextual difference of surroundings is also confirmed.

utilizes only one source domain during training. Intuitively, SSDG is more difficult to generalize successfully than MSDG because of the limited training situations. Existing SSDG models have been developed by applying data augmentation techniques to the source domain and expecting to make a robust dataset [18, 19, 20, 1]. The landmark works are ADA [20] and M-ADA [1], which use adversarial data augmentation techniques to conduct pixel-level additive perturbation.

On top of that, the maximization of diversity has been widely explored to boost generalization effects. [19, 21, 22, 23, 24] ALT [21] produces diverse images using a separate diversity module that combines augmentation such as Augmix [23] and RandConv [25]. However, from the standpoint of lane detection fields, these augmentation techniques are insufficient to contain a complex and dynamic driving environment. Therefore, in this work, we propose a method of selecting a core set that can maximize the diversity of lane structures and surroundings for generalizing lane detection models.

C. HD maps

HD maps are widely recognized for their ability to provide accurate and detailed semantic information about road environments in a machine-readable form. Despite being represented in a lightweight vector map format, HD maps contain detailed and accurate information about the road environment. This information is primarily used for vehicle localization and control [26]. Recently, there has been a growing interest in the rich semantic information contained in HD maps, and several studies [27, 28, 29] have utilized them for various other tasks beyond localization and control. Similarly, our study also utilizes road information from HD maps to improve the generalization performance of lane detection.

III. METHOD

A. Domain discrepancy in lane detection

We first explored the cause of domain discrepancy that occurs in lane detection environments. After we observed various factors, we divided the cause of the above domain discrepancy into (i) *lane structures* and (i) *surroundings*.

For lane structures, we compared the number of lanes included in each scene and curvatures as shown in Fig 2-(a). Especially, for detecting lane curvatures, we used the pre-released bezier control points [31] to calculate the bezier coefficients which represent the curvature of lanes. These plots faithfully demonstrate that the difference in lanes can be one of the factors of the domain discrepancy in lane detection scenarios. In addition, as shown in Fig 2-(b), we conducted a t-SNE [30] analysis to observe differences in surroundings. We first extracted image features from ResNet-18 and reduced the dimension via t-SNE. As shown in the result, images from the two datasets form distinctly separate clusters in the feature space.

B. Preliminaries

We propose a framework for enhancing the generalization performance of lane detection models using HD maps and image generation models. As shown in Fig. 3, we describe the proposed framework in several phases. We first extract lane markings and images from HD maps and generate realistic scenes to help with training lane detection models. At each phase, we try to enhance the diversity of lane structures and surroundings which we consider two main factors for domain discrepancy in lane detection.

Problem definition. For the Single-Source Domain Generalization(SSDG) setting for lane detection, we use source domain dataset D_s which consists of pairs of driving environment image and lane marking. Our work demonstrates HD maps can be a successful source domain for mitigating domain discrepancy in lane detection environments. To train the lane detection model as robustly as possible for the several unseen target domains D_t , we propose a diversity-targeted framework by using HD maps. More specifically, we extract the core set D_s^* of augmented samples maximizing the diversity of surroundings and lane structures.

Data selection algorithm. In this paper, we define *maximal diversity* as *minimum sum of similarities* between nodes in a graph. Let's assume a complete weighted graph $G = (V, E, W)$ where the vertex set $V = \{v_1, v_2, \dots, v_N\}$ represents N data points, and each data point is connected to every other data point through an edge $E = \{(v_i, v_j)\}$. The weight of each edge $W = \{w(i, j)\}$ is defined as the similarity between the two data points connected by the edge. The near-optimal solution can be configured as Algorithm 1. This can be freely applied to various types of data by defining only a simple metric, so it can be applied regardless of lane structure and surrounding image. Next, we define each of the similarity functions to utilize for maximal diversity selection below.

C. Increasing the diversity of lane structures

Lane mask extraction from HD map. We especially leverage the lane-related information in HD maps to construct our framework. Using the camera parameters of pre-built HD maps, we can generate the lane label masks by projecting the lane objects in HD maps within the camera view at the current location onto the camera image plane.

It is worth noting that this process does not require any additional annotation to obtain the pixel-level positions of the lane markings on the image plane. Therefore, we can acquire a substantial number of lane-label masks from HD maps.

Selection with lane structures similarities. We propose a lane similarity function s between two lane label masks $\mathbf{M}_i, \mathbf{M}_j$ that can take into account the number of lanes and curvature. We first simplify the problem by defining the similarity between the projections of each lane mask ℓ onto the image plane. We plan to use the method proposed by [32] to compare the similarity between lane curves represented in pixel coordinates.

First, we express a lane as a set of 2D points uniformly sampled along the vertical direction in the image plane, i.e., $\ell = [x_1, x_2, \dots, x_N]^T$, where x_i denotes the x -coordinate of the i -th sample, and N is the number of samples. We construct a lane matrix $\mathbf{A} = [\ell_1, \ell_2, \dots, \ell_L]$ by utilizing all L lane curves from the entire training data. By applying the SVD algorithm to the constructed lane matrix \mathbf{A} , we can factorize it as follows:

$$\mathbf{A} = \mathbf{U}\Sigma\mathbf{V}^T, \quad (1)$$

where $\mathbf{U} = [\mathbf{u}_1, \dots, \mathbf{u}_N]$ and $\mathbf{V} = [\mathbf{v}_1, \dots, \mathbf{v}_L]$ are orthogonal matrices, and Σ is a singular value matrix. Therefore, each lane curve ℓ can be approximated using M -rank approximation with singular vectors $\mathbf{u}_1, \dots, \mathbf{u}_M$ as follows:

$$\tilde{\ell}_i = \mathbf{U}_M \mathbf{c}_i = [\mathbf{u}_1, \dots, \mathbf{u}_M] \mathbf{c}_i. \quad (2)$$

The coefficient vector \mathbf{c}_i of each lane curve ℓ_i in the *eigenlane* space spanned by the singular vectors $[\mathbf{u}_1, \dots, \mathbf{u}_M]$ can be expressed as follows:

$$\mathbf{c}_i = \mathbf{U}_M^T \ell_i = [c_1, \dots, c_M]. \quad (3)$$

Therefore, we simply define the similarity between two lane curves ℓ_i and ℓ_j as Euclidean distance by projecting onto the *eigenlane* space as follows:

$$d(\ell_i, \ell_j) = |\mathbf{c}_i - \mathbf{c}_j|. \quad (4)$$

Our goal is to extend the similarity between lane curves to between lane label masks. Given two lane label masks $\mathbf{M}_i = [\ell_0^i, \dots, \ell_m^i]$ and $\mathbf{M}_j = [\ell_0^j, \dots, \ell_n^j]$, each containing m and n lane curves, respectively. Assuming that $m \geq n$ always holds, we define the lane layout similarity s between lane label marks $\mathbf{M}_i, \mathbf{M}_j$ as follows:

$$s(\mathbf{M}_i, \mathbf{M}_j) = \sum_k^n \min_l d(\ell_l^i, \ell_k^j) + |m - n| \kappa, \quad (5)$$

where κ denotes the penalty constant which we describe next. We believe that the number of curves is also an important factor in determining the similarity. Therefore, when the two-lane label masks have different numbers of lane curves, we penalize their similarity by adding κ . We empirically determine the penalty constant κ from the training dataset. This indicates that we consider the number of lane curves to be an important factor affecting diversity in most cases.

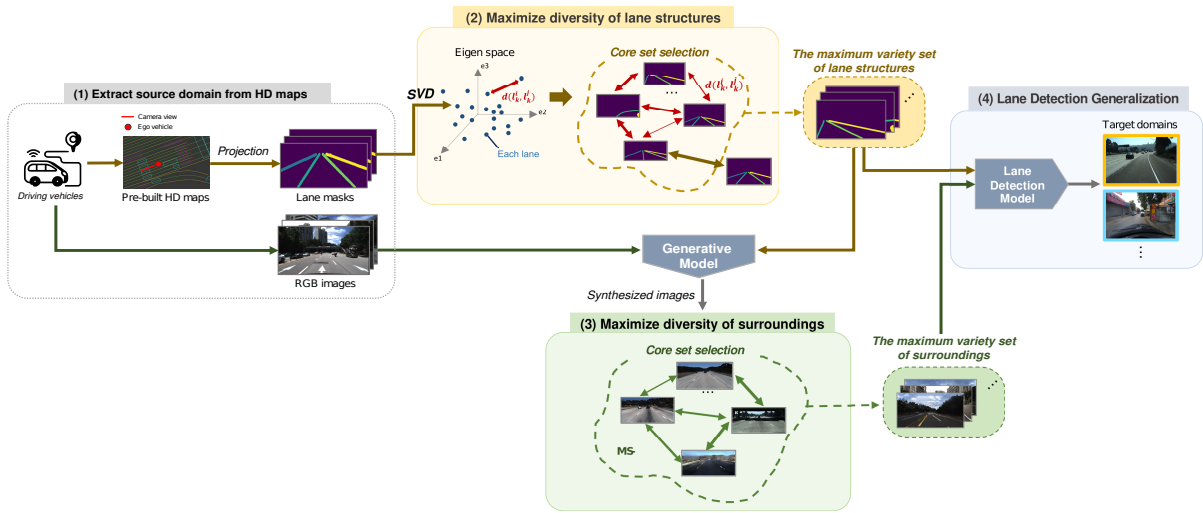


Fig. 3: **The framework of our method.** Our framework utilizes HD maps and diversity maximization methods to build robust lane detection models. (1) We first extract lane markings from HD maps and project it onto the RGB images to obtain source domain data pairs of images and lane label masks. (2) A generative model is used to synthesize diverse images corresponding to the core set of lane structures with maximal diversity, selected from the source domain data. (3) After again selecting a core set of synthesized images for each lane structure with maximal diversity, (4) we train the lane detection model and obtain enhanced domain generalization performance.

Algorithm 1 Finding a set of K vertices with the minimum sum of similarity

Require: Complete weighted graph G and $K = \#$ of vertices

- 1: Find the vertex pair (i, j) which has minimum $w(i, j)$
- 2: Add i and j to Q
- 3: **while** $|Q| < K$ **do**
- 4: Find vertex k which minimizes $\sum_{l \in V \setminus Q} w(k, l)$
- 5: **end while**

Ensure: Q

With the definition of similarity between lane label masks, we can select the K_{scene} number of masks that maximize the diversity of lane layouts by using the selection algorithm in Algorithm 1.

D. Increasing the diversity of surroundings

Selection with surrounding similarities. Our expectation is that by training the model with RGB images having identical lane labels, but different surroundings and backgrounds, the model will be less sensitive to changes in the backgrounds and surroundings. However, unlike the case of lane layouts, it is difficult to obtain a quantitative measure of the similarity between backgrounds or surroundings in RGB images. Therefore, we use a comparison metric commonly used to check the quality of generated images by image synthesis models. Therefore, we define the similarity of the surroundings in RGB images as an image metric.

The structural similarity index measure (SSIM) [33] and its multi-scale extension (MS-SSIM) [34] is a method used to compare the perceived quality of digital images and videos. They are commonly used for measuring the similarity between two images. Recently, MS-SSIM has also been

used to compare the quality of generated images against the reference images in image generation tasks [35]. Therefore, we can choose the MS-SSIM as the similarity metric between two generated images.

Finally, to train the lane detection model, we generate 100 RGB images for each lane label mask and we selected K_{image} most perceptively diverse set of generated images using MS-SSIM and the method described in Algorithm 1.

IV. EXPERIMENTS

A. Datasets

In this paper, we use three datasets for SSDG settings: LabsLane HD maps were used as the single source domain, and two commonly used benchmarks CULane and TUSimple were used as the target domain.

LabsLane: We used Naver Labs HD map¹ to create the lane label masks, which are publicly available for research purposes and provide rich information about the road environment in cities of South Korea. In order to obtain RGB images, we utilized mobile mapping vehicles equipped with high-precision RTK GPS to collect more than 100,000 images. During the projection of the lane object onto the camera view, we only considered a maximum of four lanes near the ego vehicle, which is consistent with other benchmark datasets that also have a maximum of four or five lanes. To maximize the diversity of lane layouts, we selectively sampled only the data that exhibited minimum similarity and removed duplicates. As a result, the generated dataset, called LabsLane, consists of 7,184 RGB images and corresponding 6 DoF poses.

¹<https://naverlabs.com/en/datasets>

TABLE I: **Quantitative comparison results on CULane.** We evaluate the generalization performance on CULane from TUSimple and LabsLane respectively. †Note that we attempted to reproduce [14], but were not even able to reproduce their baseline, "Source only". Therefore, in this table, we present their results as they are reported.

Experiment setting	Trained data			Total	Normal	Crowded	Night	No line	Shadow	Arrow	Dazzle light	Curve	Crossroad
	TUSimple	CULane	LabsLane										
Source only - ERFNet	✓			24.2	41	19.6	9.1	12.7	12.7	28.8	11.4	32.6	1240
Source only - GANet	✓			30.5	50	25.5	19.6	18.5	16.8	36	25.4	34.2	7405
Source only - GANet			✓	34.9	52.4	25.9	27.1	18.8	20.3	44.5	25.9	42.7	939
Advent [36]	✓	✓		30.4	49.3	24.7	20.5	18.4	16.4	34.4	26.1	34.9	6527
PyCDA [37]	✓	✓		25.1	41.8	19.9	13.6	15.1	13.7	27.8	18.2	29.6	4422
Maximum Squares [38]	✓	✓		31	50.5	27.2	20.8	19	20.4	40.1	27.4	38.8	10324
MLDA [14]†	✓	✓		<u>38.4</u>	61.4	36.3	<u>27.4</u>	<u>21.3</u>	23.4	49.1	<u>30.3</u>	<u>43.4</u>	11386
Ours - ERFNet			✓	38.2	<u>56.8</u>	32.5	24.4	23.8	<u>22.3</u>	<u>51.2</u>	32.2	40.9	4572
Ours - GANet			✓	39.6	56.7	<u>34</u>	30.1	21.2	22	53.2	27.1	46.9	<u>1275</u>

CULane: It consists of complex *urban road environments* and 133,235 frames, of which 88,880, 9,675, and 34,680 are used for training, validation, and testing, respectively.

TUSimple: It mostly consists of *highway driving scenes* and around 7,000 video clips, each containing 20 frames, with labeled lanes on the final frame of each clip.

B. Implementation details

Training: To implement the proposed framework, we used Semantic Image Synthesis(SIS) models like OASIS [39] and Pix2PixHD [40] as generative models. Note that since we wanted to generate diverse surroundings from lane masks extracted from HD maps, we used only lane labels without using the entire semantic label like conventional SIS models.

Also, we used GANet-small [2] and ERFNet [41] as lane detection models which are respectively keypoint-based and segmentation-based. We tried to validate the versatility of our method in various types of lane detection models. To ensure a fair comparison, when we used ERFNet [41], we followed the settings of benchmark datasets proposed by the domain adaptation method, MLDA [14]. For instance, we adopted the pre-processing method proposed in MLDA when using ERFNet, which established experimental settings for the generalization of lane detections. For each model, we followed their default settings during training. Specifically, all images in each dataset were resized to 768×256 to unify the size of both dataset, and only 1-degree rotation was used for augmentation.

Evaluation: We used the official evaluation code provided by CULane and TUSimple. Also, we use F1 score and accuracy respectively to measure the performance metric for CULane and TUSimple.

C. Quantitative results

Results on CULane: In Table I, we summarize the performances of each lane detection model on CULane dataset, which includes various scenario cases. We compared our methods with domain adaptation methods such as Advent [36], PyCDA [37], Maximum Squares [38], and

TABLE II: **Quantitative results on TUSimple dataset.** We evaluate the generalization performance on TUSimple from CULane and LabsLane respectively. Note that our framework using LabsLane shows similar performance with Target only.

Experiment setting	Trained data			Acc	FP	FN
	CULane	TUSimple	LabsLane			
Source only - ERFNet	✓			60.9	31.6	55.2
Source only - GANet	✓			76.9	<u>25.8</u>	35
Target only - GANet			✓	95.9	1.97	2.62
Advent [36]	✓	✓		77.1	39.7	43.9
PyCDA [37]	✓	✓		80.9	51.9	45.1
Maximum Squares [38]	✓	✓		76	38.2	42.8
MLDA [14]	✓	✓		<u>89.7</u>	29.5	<u>18.4</u>
Ours - GANet			✓	92.4	6.7	9.4

MLDA [14]. ERFNet [41] was used for testing all of the above methodologies.

Although our approach is an SSDG approach, we observe that our total performance outperforms MLDA. In particular, the performance improvement was greater when it was not a typical surrounding scene (e.g. Night, Dazzle light). This demonstrates that our HD map-based diversity maximization framework can robustly handle large domain shifts.

Results on TUSimple: We also validated our proposed framework on the TUSimple dataset in Table II. We found that our proposed framework outperforms the domain adaptation-based methods even though we do not use target domain information. It is especially notable that both MLDA [14] and the proposed method showed significant performance improvements compared to the results on CULane dataset. We conjecture that since CULane dataset is more diverse than TUSimple, it benefits more from the diversity-enhancing stages of our proposed framework.

D. Ablation studies

Using benchmark images instead of HD maps: We also conducted experiments on benchmark images rather than HD maps to verify the efficacy of our training framework itself. We measured the performance of the model learned from TUSimple to CULane. Note that it is different from MLDA [14] setting which targets Domain Adaptation sce-

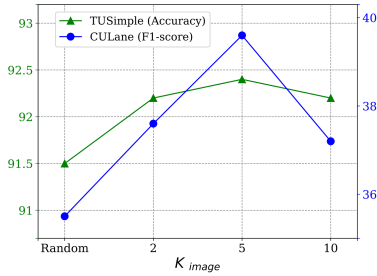


Fig. 4: **Effect of the number of selected data.** We compare the performance of randomly selecting 10 data from 100 images generated from a single lane label mask and selecting 2, 5, and 10 data using the proposed diversity-aware image selection method.

	Total	Normal	Curve
Source only (TUSimple)	24.1	41	32.6
Pix2pix [40]	26.7	43	33.2
OASIS [39]	27.3	45	37.3
OASIS + Our selection method	31.2	47.9	40.4

TABLE III: **Evaluating our methods using TUSimple images.** To verify the versatility of our framework, we tested our framework on benchmark dataset.

nario. As shown in Table III, our framework outperforms the source-only model, especially when our selection method is employed. Also, note that the performance increased for both Pix2pix and OASIS. We expect any semantic image synthesis model can be easily utilized in our framework

Effect of the number of selected images: We also experimented with the efficacy of the number of selected images. We used accuracy and total F1-score as comparison metrics for TUSimple and CULane datasets, respectively. In Fig. 4, we compare the performance of randomly selecting 10 samples from a single lane label mask of LabsLane dataset with selecting 2, 5, and 10 samples using the proposed diversity-aware image selection method. The figure shows that the proposed selection method generally outperforms random selection, and the performance is the highest when selecting 5 data for each lane label. Therefore, we set the number of synthesized data K_{image} to 5 for all experiments.

Using other image synthesis model: We also validated that our proposed framework works well with other image synthesis models. We used Pix2PixHD [40], another algorithm that can generate diverse images by re-sampling noise vectors. We trained the image synthesis model on TUSimple and evaluated the performance on total F1-score of CULane. As shown in Table III, we observed a performance improvement of about 10% when using Pix2PixHD [40] compared to training on TUSimple. However, we believe that the reason for the difference in performance is due to the quality of the generated images, as OASIS [39] produced more realistic images compared to Pix2PixHD [40].

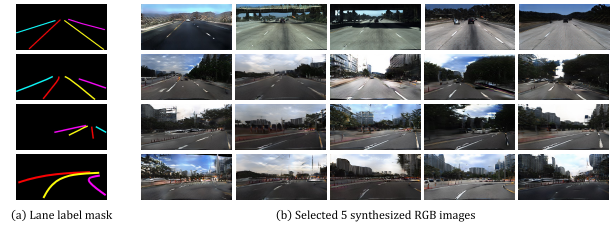


Fig. 5: **Examples of generated dataset.** We utilized OASIS as our generative model to visualize results. Our diversity maximization framework effectively helped with generating diverse surroundings.

	Source domain		Acc
	Simulator	HD map	
UNIT [13]	✓		77.5
MUNIT [42]	✓		78.6
ADA [12]	✓		82.9
Ours		✓	92.4

TABLE IV: **Results on TUSimple compared to Sim-to-Real domain adaptation.** Our performance outperforms the existing Sim-to-Real DA performance without taking advantage of any information from TUSimple.

E. Discussions

Comparison with Sim-to-Real adaptation method: The framework using HD map can be regarded as similar to the simulator in that it generates diverse augmented data. Therefore, we compared the performance on TUSimple with existing Sim-to-Real domain adaptation models [13, 42, 12] in Table IV. Their photo-realistic source domain was made by CARLA [43] which is a gaming engine to generate synthetic datasets. Note that, UNIT [13], MUNIT [42], and ADA [12] models included TUSimple’s unlabeled image as they are domain adaptation works. However, our result outperforms the existing Sim-to-Real DA performance without taking advantage of any information from TUSimple.

Comparison with cross-domain adaptation method: In Table I, we compared the proposed framework with domain adaptation methods. We confirmed that our proposed framework shows comparable results with MLDA even without any knowledge of the target domain. Furthermore, we believe that the proposed framework is not limited to a specific lane detection model but can be applied to other various lane detection models as well.

V. CONCLUSION

We propose a novel training framework that utilizes HD maps for robust lane detection. We generated a large number of images from HD maps with varying surroundings and lane structures to mitigate domain discrepancy on lane detection. Training the lane detection model with these datasets resulted in improved generalization performance. Our extensive experiments successfully demonstrate this improvement and we expect our method can be fully extended on autonomous driving scenarios.

REFERENCES

- [1] F. Qiao, L. Zhao, and X. Peng, "Learning to learn single domain generalization," in *Proceedings of the IEEE/CVF Conference on Computer Vision and Pattern Recognition*, 2020, pp. 12 556–12 565. 1, 2
- [2] J. Wang, Y. Ma, S. Huang, T. Hui, F. Wang, C. Qian, and T. Zhang, "A keypoint-based global association network for lane detection," in *Proceedings of the IEEE/CVF Conference on Computer Vision and Pattern Recognition*, 2022, pp. 1392–1401. 1, 5
- [3] D. Li, Y. Yang, Y.-Z. Song, and T. M. Hospedales, "Deeper, broader and artier domain generalization," in *Proceedings of the IEEE international conference on computer vision*, 2017, pp. 5542–5550. 1
- [4] K. Muandet, D. Balduzzi, and B. Schölkopf, "Domain generalization via invariant feature representation," in *International conference on machine learning*. PMLR, 2013, pp. 10–18. 1
- [5] H. Li, S. J. Pan, S. Wang, and A. C. Kot, "Domain generalization with adversarial feature learning," in *Proceedings of the IEEE conference on computer vision and pattern recognition*, 2018, pp. 5400–5409. 1
- [6] Q. Dou, D. Coelho de Castro, K. Kamnitsas, and B. Glocker, "Domain generalization via model-agnostic learning of semantic features," *Advances in neural information processing systems*, vol. 32, 2019. 1
- [7] Y. Li, X. Tian, M. Gong, Y. Liu, T. Liu, K. Zhang, and D. Tao, "Deep domain generalization via conditional invariant adversarial networks," in *Proceedings of the European conference on computer vision (ECCV)*, 2018, pp. 624–639. 1
- [8] G. Kang, L. Jiang, Y. Yang, and A. G. Hauptmann, "Contrastive adaptation network for unsupervised domain adaptation," in *Proceedings of the IEEE/CVF conference on computer vision and pattern recognition*, 2019, pp. 4893–4902. 2
- [9] J. Liang, D. Hu, and J. Feng, "Do we really need to access the source data? source hypothesis transfer for unsupervised domain adaptation," in *International conference on machine learning*. PMLR, 2020, pp. 6028–6039. 2
- [10] Z. Lu, Y. Yang, X. Zhu, C. Liu, Y.-Z. Song, and T. Xiang, "Stochastic classifiers for unsupervised domain adaptation," in *Proceedings of the IEEE/CVF Conference on Computer Vision and Pattern Recognition*, 2020, pp. 9111–9120. 2
- [11] C. Chen, W. Xie, W. Huang, Y. Rong, X. Ding, Y. Huang, T. Xu, and J. Huang, "Progressive feature alignment for unsupervised domain adaptation," in *Proceedings of the IEEE/CVF conference on computer vision and pattern recognition*, 2019, pp. 627–636. 2
- [12] C. Hu, S. Hudson, M. Ethier, M. Al-Sharman, D. Rayside, and W. Melek, "Sim-to-real domain adaptation for lane detection and classification in autonomous driving," in *2022 IEEE Intelligent Vehicles Symposium (IV)*. IEEE, 2022, pp. 457–463. 2, 6
- [13] M.-Y. Liu, T. Breuel, and J. Kautz, "Unsupervised image-to-image translation networks," *Advances in neural information processing systems*, vol. 30, 2017. 2, 6
- [14] C. Li, B. Zhang, J. Shi, and G. Cheng, "Multi-level domain adaptation for lane detection," in *Proceedings of the IEEE/CVF Conference on Computer Vision and Pattern Recognition*, 2022, pp. 4380–4389. 2, 5
- [15] X. Peng, F. Qiao, and L. Zhao, "Out-of-domain generalization from a single source: An uncertainty quantification approach," *IEEE Transactions on Pattern Analysis and Machine Intelligence*, 2022. 2
- [16] S. Seo, Y. Suh, D. Kim, G. Kim, J. Han, and B. Han, "Learning to optimize domain specific normalization for domain generalization," in *Computer Vision—ECCV 2020: 16th European Conference, Glasgow, UK, August 23–28, 2020, Proceedings, Part XXII 16*. Springer, 2020, pp. 68–83. 2
- [17] Q. Xu, R. Zhang, Y.-Y. Wu, Y. Zhang, N. Liu, and Y. Wang, "Simde: A simple domain expansion approach for single-source domain generalization," in *Proceedings of the IEEE/CVF Conference on Computer Vision and Pattern Recognition*, 2023, pp. 4797–4807. 2
- [18] Z. Su, K. Yao, X. Yang, K. Huang, Q. Wang, and J. Sun, "Rethinking data augmentation for single-source domain generalization in medical image segmentation," in *Proceedings of the AAAI Conference on Artificial Intelligence*, vol. 37, no. 2, 2023, pp. 2366–2374. 2
- [19] Z. Wang, Y. Luo, R. Qiu, Z. Huang, and M. Baktashmotlagh, "Learning to diversify for single domain generalization," in *Proceedings of the IEEE/CVF International Conference on Computer Vision*, 2021, pp. 834–843. 2
- [20] R. Volpi, H. Namkoong, O. Sener, J. C. Duchi, V. Murino, and S. Savarese, "Generalizing to unseen domains via adversarial data augmentation," *Advances in neural information processing systems*, vol. 31, 2018. 2
- [21] T. Gokhale, R. Anirudh, J. J. Thiagarajan, B. Kailkhura, C. Baral, and Y. Yang, "Improving diversity with adversarially learned transformations for domain generalization," in *Proceedings of the IEEE/CVF Winter Conference on Applications of Computer Vision*, 2023, pp. 434–443. 2
- [22] X. Zhang, Q. Wang, J. Zhang, and Z. Zhong, "Adversarial autoaugmentation," *arXiv preprint arXiv:1912.11188*, 2019. 2
- [23] D. Hendrycks, N. Mu, E. D. Cubuk, B. Zoph, J. Gilmer, and B. Lakshminarayanan, "Augmix: A simple data processing method to improve robustness and uncertainty," *arXiv preprint arXiv:1912.02781*, 2019. 2
- [24] S. Yun, D. Han, S. J. Oh, S. Chun, J. Choe, and Y. Yoo, "Cutmix: Regularization strategy to train strong classifiers with localizable features," in *Proceedings of the IEEE/CVF international conference on computer vision*, 2019, pp. 6023–6032. 2
- [25] Z. Xu, D. Liu, J. Yang, C. Raffel, and M. Niethammer, "Robust and generalizable visual representation learning via random convolutions," *arXiv preprint arXiv:2007.13003*, 2020. 2
- [26] J. Jeong, Y. Cho, and A. Kim, "Hdmi-loc: Exploiting high definition map image for precise localization via bitwise particle filter," *IEEE Robotics and Automation Letters*, vol. 5, no. 4, pp. 6310–6317, 2020. 2
- [27] N. Deo, E. Wolff, and O. Beijbom, "Multimodal trajectory prediction conditioned on lane-graph traversals," in *Conference on Robot Learning*. PMLR, 2022, pp. 203–212. 2
- [28] M. Heo, J. Kim, and S. Kim, "Hd map change detection with cross-domain deep metric learning," in *2020 IEEE/RSJ International Conference on Intelligent Robots and Systems (IROS)*. IEEE, 2020, pp. 10 218–10 224. 2
- [29] Q. Li, Y. Wang, Y. Wang, and H. Zhao, "Hdmapnet: An online hd map construction and evaluation framework," in *2022 International Conference on Robotics and Automation (ICRA)*. IEEE, 2022, pp. 4628–4634. 2
- [30] L. Van der Maaten and G. Hinton, "Visualizing data using t-sne." *Journal of machine learning research*, vol. 9, no. 11, 2008. 2, 3
- [31] Z. Feng, S. Guo, X. Tan, K. Xu, M. Wang, and L. Ma, "Rethinking efficient lane detection via curve modeling," in *Computer Vision and Pattern Recognition*, 2022. 3
- [32] D. Jin, W. Park, S.-G. Jeong, H. Kwon, and C.-S. Kim, "Eigenlanes: Data-driven lane descriptors for structurally diverse lanes," in *Proceedings of the IEEE/CVF Conference on Computer Vision and Pattern Recognition*, 2022, pp. 17 163–17 171. 3
- [33] Z. Wang, A. C. Bovik, H. R. Sheikh, and E. P. Simoncelli, "Image quality assessment: from error visibility to structural similarity," *IEEE transactions on image processing*, vol. 13,

- no. 4, pp. 600–612, 2004. 4
- [34] Z. Wang, E. P. Simoncelli, and A. C. Bovik, “Multiscale structural similarity for image quality assessment,” in *The Thirty-Seventh Asilomar Conference on Signals, Systems & Computers, 2003*, vol. 2. Ieee, 2003, pp. 1398–1402. 4
- [35] J. Snell, K. Ridgeway, R. Liao, B. D. Roads, M. C. Mozer, and R. S. Zemel, “Learning to generate images with perceptual similarity metrics,” in *2017 IEEE International Conference on Image Processing (ICIP)*. IEEE, 2017, pp. 4277–4281. 4
- [36] T.-H. Vu, H. Jain, M. Bucher, M. Cord, and P. Pérez, “Advent: Adversarial entropy minimization for domain adaptation in semantic segmentation,” in *Proceedings of the IEEE/CVF conference on computer vision and pattern recognition*, 2019, pp. 2517–2526. 5
- [37] Q. Lian, F. Lv, L. Duan, and B. Gong, “Constructing self-motivated pyramid curriculums for cross-domain semantic segmentation: A non-adversarial approach,” in *Proceedings of the IEEE/CVF International Conference on Computer Vision*, 2019, pp. 6758–6767. 5
- [38] M. Chen, H. Xue, and D. Cai, “Domain adaptation for semantic segmentation with maximum squares loss,” in *Proceedings of the IEEE/CVF International Conference on Computer Vision*, 2019, pp. 2090–2099. 5
- [39] V. Sushko, E. Schönfeld, D. Zhang, J. Gall, B. Schiele, and A. Khoreva, “You only need adversarial supervision for semantic image synthesis,” *arXiv preprint arXiv:2012.04781*, 2020. 5, 6
- [40] T.-C. Wang, M.-Y. Liu, J.-Y. Zhu, A. Tao, J. Kautz, and B. Catanzaro, “High-resolution image synthesis and semantic manipulation with conditional gans,” in *Proceedings of the IEEE conference on computer vision and pattern recognition*, 2018, pp. 8798–8807. 5, 6
- [41] E. Romera, J. M. Alvarez, L. M. Bergasa, and R. Arroyo, “Erfnet: Efficient residual factorized convnet for real-time semantic segmentation,” *IEEE Transactions on Intelligent Transportation Systems*, vol. 19, no. 1, pp. 263–272, 2017. 5
- [42] X. Huang, M.-Y. Liu, S. Belongie, and J. Kautz, “Multimodal unsupervised image-to-image translation,” in *Proceedings of the European conference on computer vision (ECCV)*, 2018, pp. 172–189. 6
- [43] A. Dosovitskiy, G. Ros, F. Codevilla, A. Lopez, and V. Koltun, “Carla: An open urban driving simulator,” in *Conference on robot learning*. PMLR, 2017, pp. 1–16. 6